ISSN 1547-4771, Physics of Particles and Nuclei Letters, 2024, Vol. 21, No. 4, pp. 919–927. © The Author(s), 2024. This article is an open access publication.
Russian Text © The Author(s), 2024, published in Pis'ma v Zhurnal Fizika Elementarnykh Chastits i Atomnogo Yadra, 2024.

METHODS OF PHYSICAL EXPERIMENT

Characterization of Tracking Modules Based on DSSD Sensors at the SC-1000 Accelerator for the BM@N Project

D. V. Dementev[a, *], A. D. Sheremetev[a], M. O. Shitenkov[a], V. V. Leontiev[a, b], I. A. Rufanov[a], and Yu. A. Murin[a]

[a] *Veksler and Baldin Laboratory of High Energy Physics, Joint Institute for Nuclear Research, Dubna, Moscow oblast, 141980 Russia*

[b] *Moscow State University, Moscow, 119991 Russia*

**e-mail: dementiev@jinr.ru*

Received December 8, 2023; revised February 2, 2024; accepted February 2, 2024

Abstract—The results of studying characteristics of modules based on double-sided microstrip silicon sensors, which are designed to create the wide-aperture Silicon Tracking System for the BM@N facility, are presented. The main module features are the use of fast readout electronics based on the STS-XYTER chip and the application of ultralight (0.23% X_0) aluminum microcables for transmitting analog signals from the sensor strips to the input channels of the readout electronics. The results of testing different configurations of tracking modules on the extracted beam of protons at the SC-1000 accelerator in the PNPI are presented. The stable operation of readout electronics is demonstrated at loads close to the maximum values of 360 kHz s^{-1} cm^{-2}. The signal-to-noise ratio was no less than 23. The measured coordinate resolution of the modules within the beam telescope was 17 ± 0.4 μm, and the detector efficiency of recording for protons with energy of 1 GeV was no less than 99%.

DOI: 10.1134/S1547477124701000

INTRODUCTION

The BM@N facility is the first physics experiment at the NICA accelerator complex, which is currently under construction at the Joint Institute for Nuclear Research. The main goal of the experiment is to study the properties of superdense baryonic matter in collisions of gold nuclei with energies up to 3.8 GeV/nucleon [1]. To accurately measure the momenta of decay products of multistrange hyperons and hypernuclei, it is planned to upgrade the hybrid tracking system. The facility upgrading involves the integration of additional four planes of a silicon track system (STS) based on double-sided silicon strip detectors (DSSD) with fast readout electronics [2]. The intensity of gold ion beams at the facility will be up to 10^6 ion/s [3]. High intensities of beams, as well as the multiplicity of secondary particles produced in heavy-ion interactions, impose additional requirements on the processing rate of data coming from detectors and the speed of readout electronics.

One possible way to solve this problem is to abandon the traditional architecture of the experimental data acquisition system, based on the use of a hardware trigger signal, and to move to the method of data streaming with the subsequent frame-by-frame processing of events. The streaming architecture uses the principle of parallel signal processing and formation of an independent trigger in each individual channel. Information from the detector readout electronics is transmitted in a continuous stream. For further processing, the data are sorted based on the time stamp, and the timeslices of a given size are formed. Then they are transferred to the computing center, where the timeslice-based parallel processing, the online event reconstruction, and selection occur on the basis of the 4D tracking algorithms [4].

The first tracking modules based on DSSD sensors with the readout electronics, having a streaming architecture of data transmission, were developed for the CBM STS project [5] and intended to operate on a heavy-ion beam with an intensity of up to 10 MHz under conditions of a high multiplicity of secondary particles (up to 700 particles). The design of this module and readout electronics was optimized for using in the BM@N STS project [6]. This work presents the results of studying a number of characteristics of BM@N track modules necessary for operation in the experiment.

DESIGN OF THE BM@N DSSD MODULE

The BM@N silicon track system should consist of four layers based on 292 DSSD modules. The STS project is described in detail in [7, 8]. The track module shown in Fig. 1 is a key element of the design and

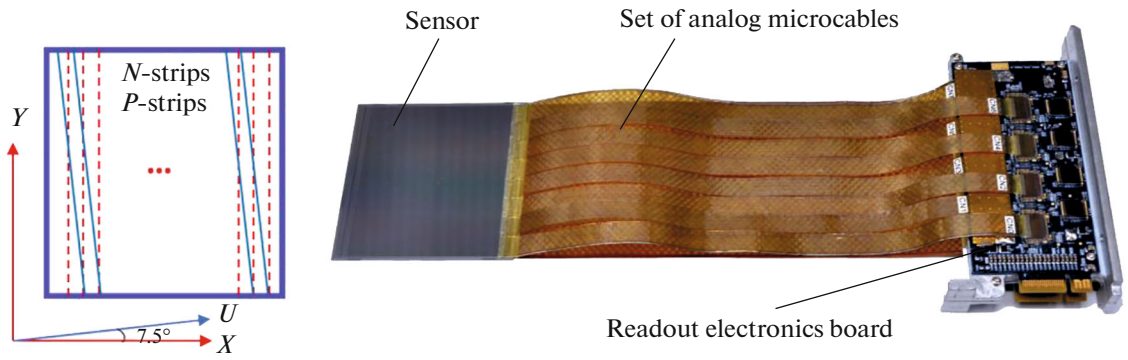

Fig. 1. DSSD module of BM@N STS. A diagram of the arrangement of strips on the sensor is shown on the left. Arrows indicate directions of the axes used in the text. A photograph of the assembled module is shown on the right.

consists of a double-sided microstrip silicon sensor, two boards with readout electronics for reading and processing signals, and a set of ultralight aluminum microcables connecting the sensor strips to the input channels of readout electronics.

The thickness of the sensors is 320 ± 15 μm. On each side of the sensor, there are 1024 strips at a pitch of 58 μm. The strips on the N- and P-sides of the sensor are located at an angle of 7.5°, thereby forming a spatial grid with cell sizes Δx = 58 μm and Δy = 58 μm/tan(7.5°) = 440.6 μm. The layout of the strips is shown in Fig. 1. A set of 16 microcables of 64 channels each is used to connect each side of the sensor to the readout electronics. The signal line of the microcable is an aluminum track with a thickness of 10 μm and a width of 116 μm; the parasitic capacitance of the track is 0.5 pF/cm. The total thickness of the microcable is 0.23% X_0. The use of these analog loops makes it possible to localize the detector readout electronics in the peripheral area of the station, by minimizing, in this case, the amount of substance in the sensitive area of the tracking system and the radiation background in the area where the electronics is located [7].

The module can be complemented, depending on its location in the track plane, with a different set of components. The sensor size can be 62 × 62 mm or 42 × 42 mm; the microcable lengths can vary from 110 to 280 mm. Modules located close to the beam axis have a smaller size of sensor (strip area) in order to minimize detector loads. At the same time, a set of microcables of greater length is used in the central modules, since the readout electronics are located in the edge areas of tracking stations. The module design and the assembly process are described in detail in [2, 9].

The readout electronics of the module is implemented on STS-XYTER ultrafast application-specific integrated circuits (ASICs) [10] and is described in [11]. This ASIC is based on a streaming data processing architecture that allows operation without data loss with an average channel load of up to 250000 events per second at a maximum clock frequency of 160 MHz and with the utilization of five synchronous data lines per chip. This high operating speed is ensured by the use of trigger-free data transfer logic, analog signal generation time of up to 80 ns, and the use of separate 5-bit ADCs in each of the 128 channels of the chip.

The price for the high throughput of the detector's readout electronics is a limitation on the transmission distance of the high-frequency digital signal, as well as a large volume of cables when using several parallel transmission lines for each chip. In the STS data acquisition system, the operating mode of the detector readout electronics is selected based on the results of a computer simulation of the tracking system loads, which will be no more than 150 Hz/channel [8]. In STS track modules, the throughput of STS-XYTER chips is 12e500 events per channel per second. The throughput limitation is due to the use of a lower clock frequency of 40 MHz for data transmission over a long cable (up to 10 m) and a single data line per chip [12]. The architecture of the BM@N STS data acquisition system is described in detail in [13].

The parameters of the STS module must satisfy the following requirements [8]:

(i) reading and processing the signals from the detector under conditions of loads up to 5 kHz/cm^2 or 150 Hz/channel;

(ii) signal-to-noise ratio of no less than 10;

(iii) spatial resolution no worse than 30 μm;

(iv) no more than 3% of idle channels;

(v) stable operation with an equivalent neutron fluence of 10^{11} n_{eq}/cm^2.

Within the preseries assembly, eight modules were assembled at the building bay of the Veksler and Baldin Laboratory of High Energy Physics, Joint Institute for Nuclear Research, some of which were tested on an extracted proton beam at the SC-1000 accelerator in March 2023.

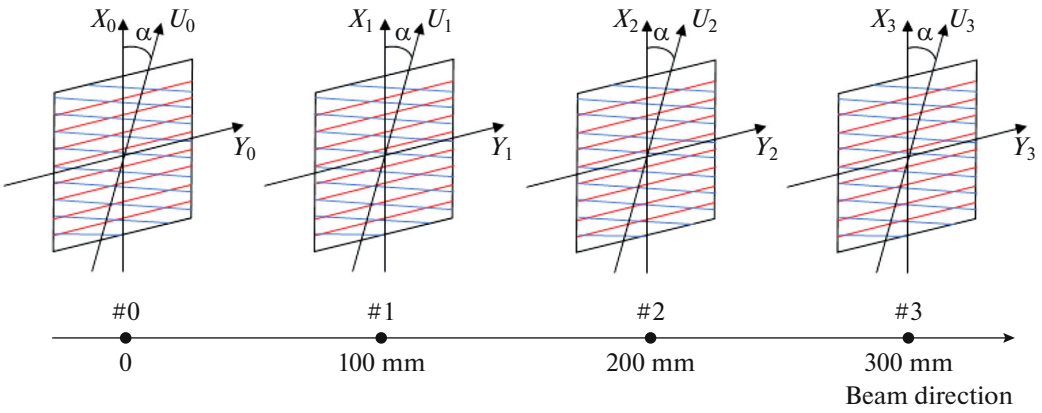

Fig. 2. Telescope based on DSSD modules for the BM@N project. A diagram of the arrangement of sensors along the beam axis is shown on the top. The color red indicates the direction of the strips on the N-side, and blue indicates the direction of the strips on the P-side. The directions of the coordinate axes used in the text are given. The telescope image is shown on the bottom.

TEST BENCH

The bench for testing modules on the extracted beam of the SC-1000 accelerator was a beam telescope based on four track modules. To generate a trigger signal, two additional scintillation counters were utilized which were installed in front and behind the telescope. The trigger signal was used to selectively record events selected from the overall data stream transmitted by the detector's readout electronics. The measurements were performed on a proton beam with an energy of 1 GeV and an intensity from 10^4 to 3×10^5 protons per second per cm^2. The bench diagram is shown in Fig. 2.

All four modules have sensors measuring 62 × 62 mm (sensitive area size is 60 × 60 mm). A length of microcables for modules no. 0, 1, and 2 is 117 mm and, for module no. 3, 155 mm. The sensors are installed at a pitch of 100 mm along the beam axis. In this work, the following parameters of the modules were studied: signal-to-noise ratio, stability of the readout electronics under conditions of maximum detector loads, spatial resolution, and efficiency of particle recording.

RESULTS OF FIELD TESTS

1. Throughput of the Detector Readout Electronics

The operating principle and signal generation circuit in the channel of the STS-XYTER chip are described in [10]. STS-XYTER implements the principle of parallel data processing, in which a trigger is generated independently by each channel when the amplitude of the input signal exceeds the specified threshold of the comparator. The event information transmitted to the chip output contains 14 bits of a time stamp and 5 bits of signal amplitude. At the channel input there is a charge-sensitive amplifier (CSA), the output signal of which is transmitted to two shaper amplifiers. A fast shaper amplifier and a discriminator are used to generate a time stamp. A slow shaper amplifier and ADC are used to measure the signal amplitude. If a signal arrives at the channel input while the previous event is being processed (before it is written to the FIFO buffer or if the buffer is full at that moment), then the new event is lost and the *Event-Missed* flag is set to 1.

The throughput of the STS-XYTER chip when operating at a clock frequency of 40 MHz is $F_{\text{ASIC}} =$ 1.6 million events per second (12e500 events per channel per second). One chip processes data from a sensor area of 7.4 × 60 mm (4.4 cm^2), so the maximum permissible detector load is $F_{\text{ASIC}}/4.4 = 360000$ events/cm^2. During operation at the accelerator, the operation of the readout electronics was tested under conditions of various loads up to 3×10^5 particles s^{-1} cm^{-2}; the beam diameter was ~2 cm. To measure the beam intensity, both the readings from an ionization chamber installed in front of the beam telescope and the analysis of data from track modules were used.

To integrate the STS readout electronics into the BM@N global data acquisition system, the ability to select events based on the arrival of an external trigger signal was implemented. The event selection is implemented in FPGA-based electronic modules that receive and process information from the detector readout electronics. This filter allows a time window of a given size W to be "cut" from a continuous data stream (Fig. 3). The chip load F in this operating mode can be estimated as

$$F = \frac{f}{N_{\text{tg}} W}, \tag{1}$$

where f is the number of hits transmitted by the chip in one second; N_{tg} is the number of trigger signals received by the chip in 1 s. The time window size in all tests was $W = 0.5$ μs. The trigger system was configured so that a time interval between adjacent trigger signals was at least 20 μs. The results are presented in

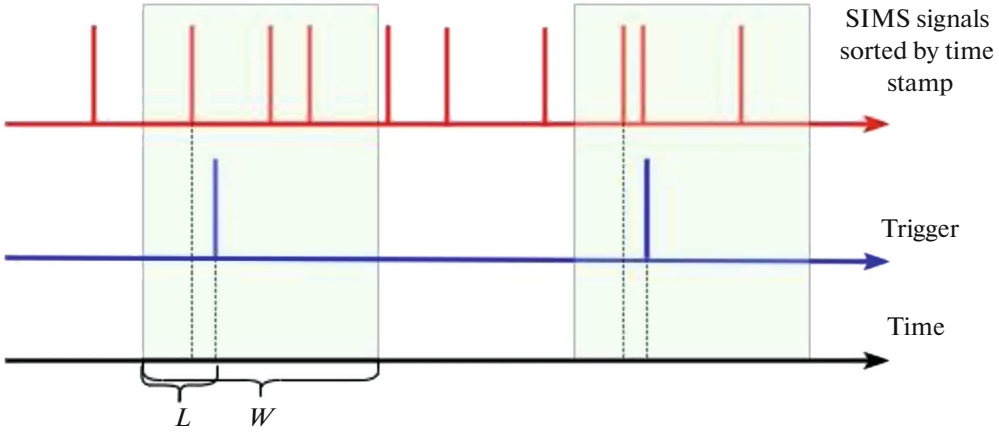

Fig. 3. Scheme for forming a time window based on a trigger signal. The red line shows signals coming from SIMS, which were sorted by time stamp. The time window (shown as green rectangles) is formed on the basis of the trigger signal (shown with a blue line). The trigger delay (L) and time window width (W) parameters are user-defined.

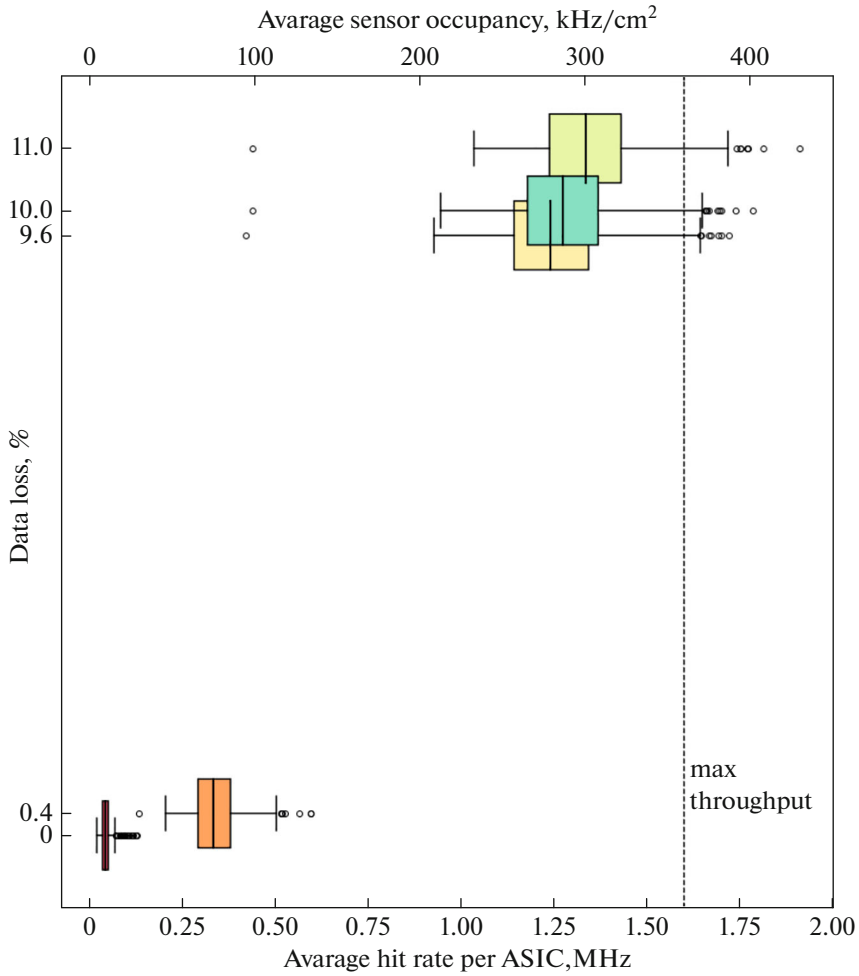

Fig. 4. Dependence of the amount of lost data on the load of the STS XYTER chip. The vertical line indicates the limiting throughput.

Fig. 4. The maximum frequency of events processed by one chip in the experiment was 1.3 million per second, which corresponds to a detector load of 295 500 events/cm^2. With these beam parameters, a volume of data loss (a number of events with *Event-Missed* = 1) was 11%. Partial losses in this case are due

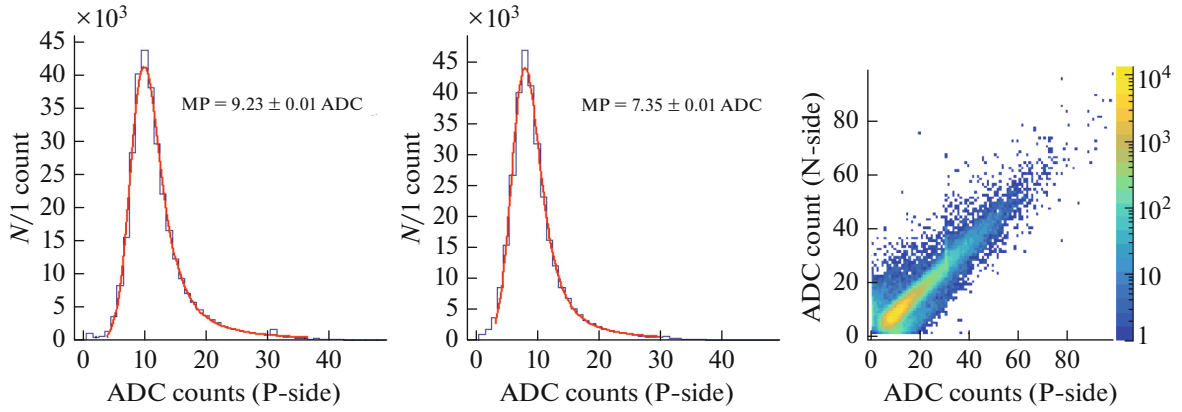

Fig. 5. Distribution of signal amplitudes for module 1 in units of ADC counts. Distributions for P- and N-sides are given on the left; red lines show the result of data approximation by convolution of Gaussian and Landau functions. Correlations between the amplitudes of signals from a single particle on both sides of the module are shown on the right.

to the nonuniformity of the beam intensity: the standard deviation of the chip load distribution during one data set is 155000 per second. Insignificant data loss (less than 1%) is also observed at lower loads: about 400 kHz s^{-1} (91 kHz s^{-1} cm^{-2}). Apparently, these losses are due to short intensity peaks during accelerator operation.

The readout electronics throughput of the track module significantly exceeds the requirements of the BM@N experiment, which amount to 19200 events per second for one chip. The throughput of the STS module readout electronics can be additionally increased by a factor of four without modifying the design by increasing the carrier frequency of the data transmission line up to 160 MHz. This makes it possible to use BM@N track modules both under conditions of more intense beams at the NICA accelerator complex and in other experiments using high-intensity heavy ion beams, such as CBM.

2. Signal-to-Noise Ratio

The signal-to-noise ratio (S/N) for STS track modules is determined as follows. The noise (N) is an average value of the equivalent noise charge in the secondary ion mass spectrometer (SIMS) channels. The greatest influence on the noise amplitude is exerted by the capacitance at the input of the SIMS CSA [14]. The signal (S) is the most probable amplitude value of the charge signal in the detector from a minimally ionizing particle (MIP). For protons, the minimum ionizing ability corresponds to an energy of ~2.45 GeV [15]. In this work, measurements were performed using a proton beam with an energy of 1 GeV. The signal from MIP was calculated as follows [15]:

$$S = 0.92MP, \quad (2)$$

where MP is the measured most probable value of the signal amplitude in the detector from protons with an energy of 1 GeV. Figure 5 shows the distributions of the measured signals for both sides of module no. 1 and also shows the correlations between the amplitudes of signals on both sides of the sensor.

The results of an estimation of the average equivalent noise charge (N) and the most probable value of the signal amplitude (S) are given in Table 1. The error in estimating signal amplitudes is primarily due to the accuracy of calibration of the analog paths of the chip, which is 3%. The range of signal-to-noise ratio values for P-sides of the sensors was 26.7–32.1 and for N-sides it was 23.4–25.3.

Table 1. Signal-to-noise ratio for tested modules. The values of N_P, N_N are the average values of the equivalent noise charge ("noise") on the corresponding sides of the sensor; S_P and S_N are the average signal amplitudes. Values are given in units of thousands of electrons. The S/N ratio is indicated in terms of the IFM signal

ID	S_P [$\times 10^3$ e^-]	N_P [$\times 10^3$ e^-]	S_N [$\times 10^3$ e^-]	N_N [$\times 10^3$ e^-]	S_P/N_P	S_N/N_N
0	26.3 ± 0.9	0.82 ± 0.07	22.3 ± 0.8	0.88 ± 0.07	32.1 ± 1	25.3 ± 0.8
1	25.7 ± 0.9	0.83 ± 0.07	22.2 ± 0.8	0.86 ± 0.07	31.0 ± 1	25.8 ± 0.8
2	25.7 ± 0.9	0.79 ± 0.07	22.8 ± 0.8	0.85 ± 0.07	32.5 ± 1	26.8 ± 0.9
3	25.4 ± 0.9	0.95 ± 0.08	21.8 ± 0.8	0.930 ± 0.08	26.7 ± 0.9	23.4 ± 0.8

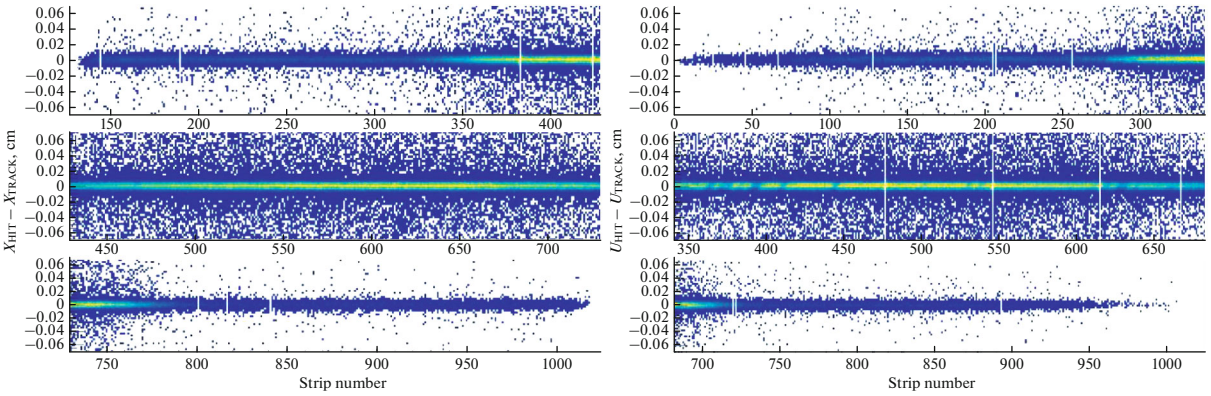

Fig. 6. Distribution of track residuals across channels for module 1 on the N-side (on the left) and P-side (on the right).

3. Spatial Resolution

All modules of the telescope shown in Fig. 2 have the same structure with horizontal strips measuring the X coordinate on the N-side, and U strips tilted at a stereo angle of 7.5° on the P-side. The X strips of different modules are located parallel (as are U strips). Combinations of intersecting X and U clusters in the module determine the Y coordinates of the particle impact point.

The estimation of STS module parameters requires the precision geometric reconstruction of tracks in the beam telescope. Before it is carried out, the map of correspondence between the positions of the module strips and the numbers of the corresponding electronic channels of the readout electronics is checked and, if necessary, corrected. First and foremost, the correlations of the numbers of triggered strips on each side of the module are considered. Since about 2% of clusters consist of a pair of strips, simultaneous activations of neighboring channels clearly stand out against the background of random coincidences. For a final check of the map, it is enough to compare the number of the triggered strip with the track prediction that was performed through a couple of other modules in ZX or ZU projections. An example of this comparison is shown in Fig. 6. The absence of outbreaks and ladders in this distribution confirms that the channel map is correct.

To carry out precision geometric reconstruction, let us imagine the telescope (Fig. 2) as a system of two modules with numbers 0 and 2, used to construct direct tracks and modules 1 or 3, in which the spread of track misses σ_{res} relative to the points measured in it is estimated. A coordinate system is selected in which modules 0 and 2 are located in accordance with geodetic measurements, and the positions of modules 1 and 3 are adjusted mathematically. In an ideally geometrically aligned system, the spread of track misses σ_{res} depends on the resolution of the detector σ_d, the accuracy of carrying out the direct track σ_t, and the deviation of the track due to multiple Coulomb scattering σ_{mcs} as

$$\sigma_{res} = \sigma_d \oplus \sigma_t \oplus \sigma_{mcs}. \quad (3)$$

The accuracy of the track reconstruction depends in this case both on the location of the plane on which the track is projected and on the spatial resolution of the modules, based on whose hits the track line is drawn.

Let two planes with coordinates z' and z'' along the beam be used to construct the track, while the third, test plane, be used to determine the residual σ_{res}. The accuracy of drawing the track to point z, provided that the spatial resolution of all modules is the same and equal to σ_d, is

$$\sigma_t^2(z) = \frac{\sigma_d^2}{2}\left(1 + 4\left(\frac{z - (z'' + z')/2}{z'' - z'}\right)^2\right) = K(z)\sigma_d^2, \quad (4)$$

where coefficient K depends on the relative position of the modules. In this analysis, planes 0 ($z' = 0$ mm) and 2 ($z'' = 200$ mm) were used to carry out the construction of tracks; residuals were calculated for planes 1 ($z = 100$ mm) and 3 ($z = 300$ mm), for which coefficient K was 0.5 and 2.5, respectively.

From Eqs. (3) and (4) it follows that the spatial resolution of the modules can be calculated as follows:

$$\sigma_d = \frac{\sqrt{\left(\sigma_{res}^2 - \sigma_{mcs}^2\right)}}{\sqrt{(K(z)+1}}. \quad (5)$$

The distribution of track residuals for modules 1 and 3 is given in Fig. 7.

The effect of multiple Coulomb scattering on the track residual can be determined using the formula for the average scattering angle [16]:

$$\sigma_\theta = \frac{13.6}{\beta cp\,[\mathrm{MeV}]}\sqrt{\frac{X}{X_0}}\left(1 + 0.038\ln\left(\frac{X}{X_0}\right)\right). \quad (6)$$

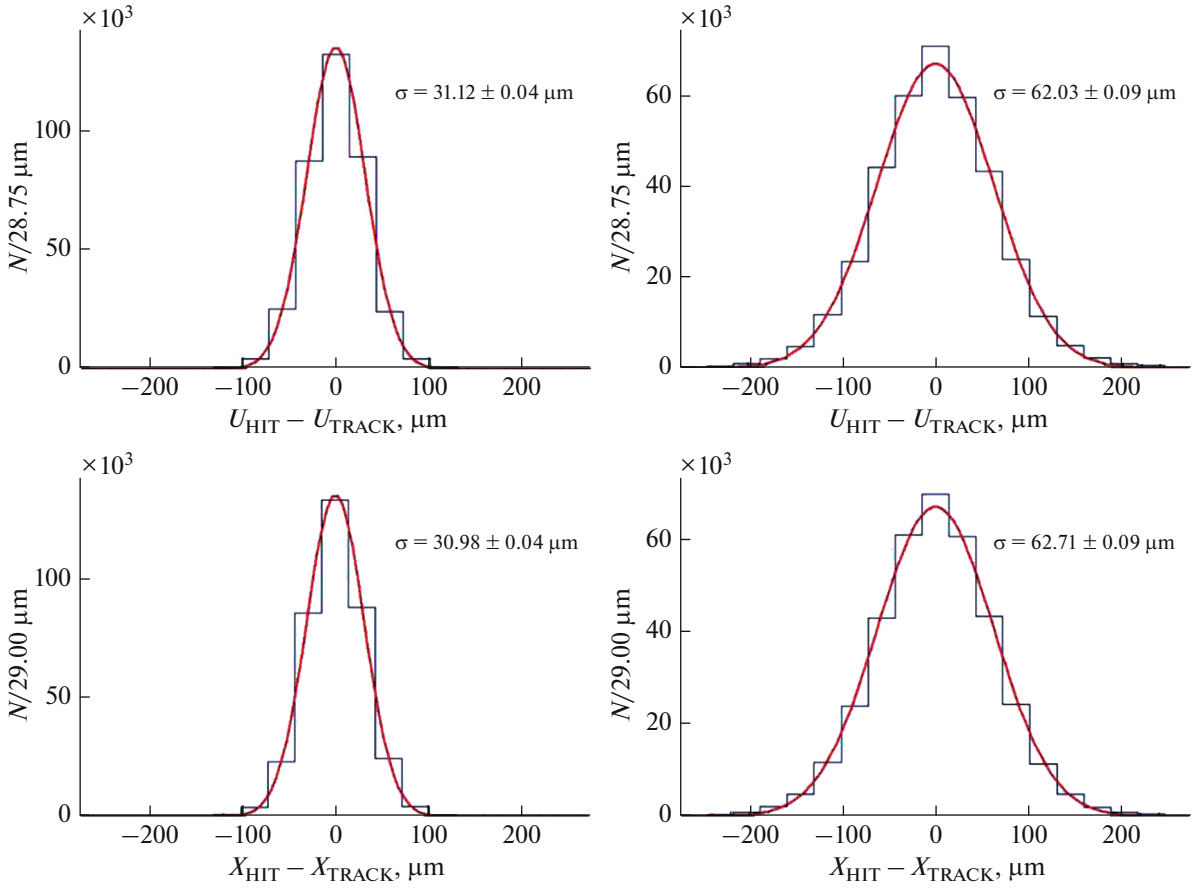

Fig. 7. Distribution of track residuals ΔX and ΔU for modules 1 (on the left) and 3 (on the right).

The thickness of each module is $X/X_0 = 0.38 \pm 0.01\%$. For planes 1 and 3, $\sigma_{mcs} \sim \sigma_\theta L$, where $L = 100$ mm is the distance between the planes. To estimate σ_{mcs}, the Monte Carlo simulation was performed in the GEANT4 software environment, the results of which are shown in Fig. 8.

The calculated values of the spatial resolution of the modules in the XU coordinate system are presented in Table 2. The values obtained during the analysis of track residuals in planes 1 and 3 coincide with each other and correspond to the theoretical estimate of the coordinate resolution of the sensor with strip pitch $p = 58$ μm, which is $p/\sqrt{12} = 16.7$ μm. The main contribution to the calculation error of σ_{mcs} is determined by the accuracy of measuring the distance between planes and by the spread of the thicknesses of sensors.

4. Detection Efficiency

To assess the efficiency of detecting protons with an energy of 1 GeV by the sensor, the distribution of relative track residuals in the XY coordinate plane for module 1 was constructed, which were determined by the following formula:

$$\delta^2 = \frac{dx^2}{\sigma_{x_1}^2} + \frac{dy^2}{\sigma_{y_1}^2}, \quad (7)$$

where $\sigma_{x_1} = 31$ μm, $\sigma_{y_1} = 194$ μm are the track residuals for the first station in XY coordinates. The resulting distribution is shown in Fig. 9. If there was no hit corresponding to a given track in the sensor under study, the event was written into the last bin of the histogram. It is important to note that zones with nonworking and adjacent channels on the sensors were excluded from this analysis. Less than 0.5% of events

Table 2. Spatial resolution of modules σ_d, obtained by analyzing track residuals for planes 1 and 3 of the beam telescope

Coordinate	σ_{res}, μm	σ_{mcs}, μm	σ_d, μm
X_1	30.98 ± 0.04	23.3 ± 0.4	16.7 ± 0.4
U_1	31.12 ± 0.04	23.3 ± 0.4	16.9 ± 0.4
X_3	62.03 ± 0.09	53.3 ± 0.9	16.9 ± 0.8
U_3	62.71 ± 0.09	53.3 ± 0.9	17.6 ± 0.8

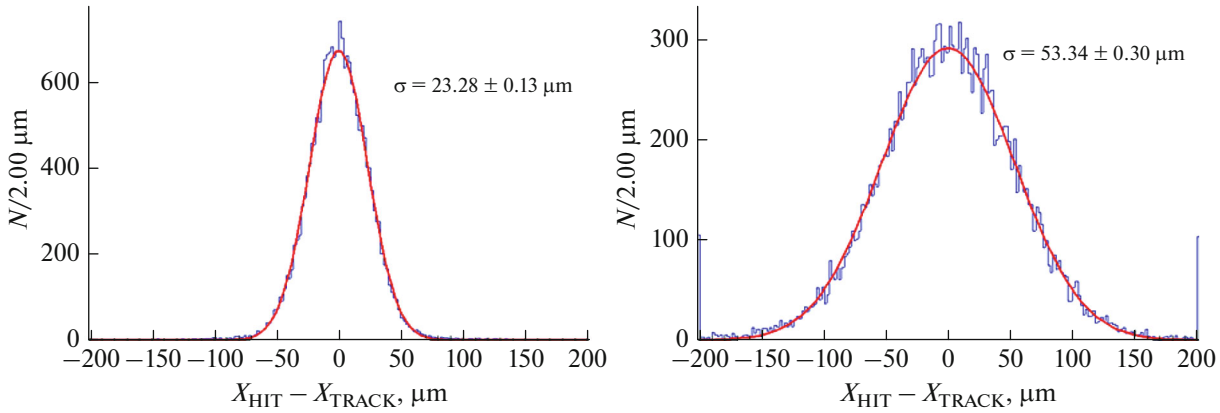

Fig. 8. Results of Monte Carlo simulation of the track residual σ_{mcs} for planes 1 (on the left) and 3 (on the right) due to the multiple Coulomb scattering.

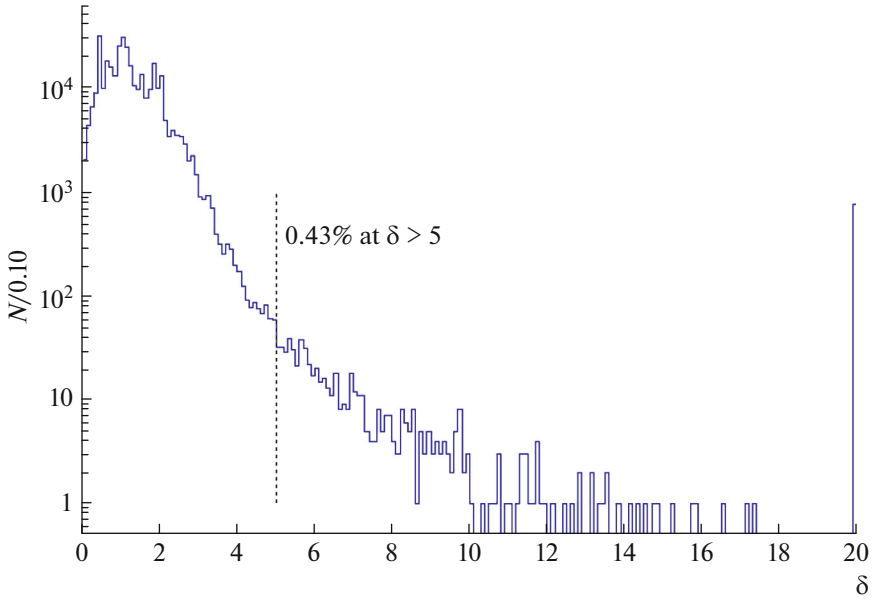

Fig. 9. Distribution of relative track residual for module 1.

belong to the range $\delta > 5$. Thus, the detection efficiency of sensors for protons with an energy of 1 GeV in the described experiment was no less than 99% for those areas where all channels are operational.

CONCLUSIONS

The characteristics of DSSD modules for the BM@N silicon track system were studied using an extracted beam of protons with an energy of 1 GeV. In the process of field measurements, the following results were obtained. The signal-to-noise ratio for modules of various configurations (microcable length of 110 and 155 mm) ranged from 23 to 32. The coordinate resolution of the sensors was 17 ± 0.4 μm. The efficiency of detecting particles with a single detector was 99% for the areas where all channels were operational. The readout electronics of the modules demonstrated a stable operation under conditions of the detector load up to 295 kHz s^{-1} cm^{-2}. The values satisfy with a margin the necessary requirements for the BM@N silicon track system. The high throughput of the readout electronics makes it possible to use these track modules in future experiments under significantly higher load conditions.

ABBREVIATIONS AND NOTATION

ADC	Analog to Digital Converter
ASIC	Application Specific Integrated Circuit
BM@N	Baryonic Matter at Nuclotron
CBM	Compressed Baryonic Matter
CSA	Charge-Sensitive Amplifier
DSSD	Double-Sided Silicon Detector
FPGA	Field-Programmable Gate Array

IFM	Instantaneous Frequency Measurement
MIP	minimally ionizing particle
NICA	Nuclotron-based Ion Collider Facility
PNPI	Petersburg Nuclear Physics Institute
SC	synchrocyclotron
SIMS	Secondary Ion Mass Spectrometer
STS	Silicon Tracking System

FUNDING

This work was supported by ongoing institutional funding. No additional grants to carry out or direct this particular research were obtained.

CONFLICT OF INTEREST

The authors of this work declare that they have no conflicts of interest.

OPEN ACCESS

REFERENCES

1. V. D. Kekelidze, "NICA project at JINR: status and prospects," J. Instrum. **12**, C06012 (2017). https://doi.org/10.1088/1748-0221/12/06/C06012
2. P. Senger, D. Dementev, J. Heuser, M. Kapishin, E. Lavrik, Y. Murin, A. Maksymchuk, H. R. Schmidt, C. Schmidt, A. Senger, and A. Zinchenko, "Upgrading the baryonic matter at the Nuclotron experiment at NICA for studies of dense nuclear matter," Particles **2**, 481—490 (2019). https://doi.org/10.3390/particles2040029
3. M. Kapishin (BM@N Collab.), "Studies of baryonic matter at the BM@N experiment (JINR)," Nucl. Phys. A **982**, 967—970 (2019). https://doi.org/10.1016/j.nuclphysa.2018.07.014
4. V. Akishina and I. Kisel, "Parallel 4-dimensional cellular automaton track finder for the CBM experiment," J. Phys.: Conf. Ser. **762**, 012047 (2016). https://doi.org/10.1088/1742-6596/762/1/012047
5. A. Rodríguez Rodríguez, O. Maragoto Rodríguez, J. Lehnert, A. Toia, M. Teklishyn, A. Lymanets, D. Rodríguez, J. M. Heuser, and C. J. Schmidt, "Functional characterization of modules for the silicon tracking system of the CBM experiment," Nucl. Instrum. Methods Phys. Res., Sect. A **1058**, 168813 (2024). https://doi.org/10.1016/j.nima.2023.168813
6. A. D. Sheremetyev, D. V. Dementyev, V. V. Leontiev, M. O. Shitenkov, and Yu. A. Murin, "Technological process of assembling and testing track modules based on silicon double-sided microstrip detectors," Pis'ma EChAYa 21, No. 3 (2024).
7. D. Dementev, A. Baranov, V. Elsha, et al., "The silicon tracking system as a part of hybrid tracker of BM@N experiment," Phys. Part. Nucl. **53**, 197—202 (2022). https://doi.org/10.1134/S1063779622020265
8. D. Dementev, A. Baranov, V. Elsha, et al., The silicon tracking system as a part of hybrid tracker of BM@N experiment," Technical Design Report (JINR, Dubna, 2020).
9. A. Sheremetev et al., "The quality assurance test system for assembly of STS modules for the BM@N experiment," Phys. Part. Nucl. **20**, 613—618 (2023). https://doi.org/10.1134/S1547477123040593
10. K. Kasinski, A. Rodriguez-Rodriguez, J. Lehnert, W. Zubrzycka, R. Szczygiel, P. Otfinowski, R. Kleczek, and C. J. Schmidt, "Characterization of the STS/MUCH-XYTER2, a 128-channel time and amplitude measurement IC for gas and silicon microstrip sensors," Nucl. Instrum. Methods Phys. Res., Sect. A **908**, 225—235 (2018). https://doi.org/10.1016/j.nima.2018.08.076
11. M. Shitenkov, D. Dementev, A. Voronin, et al., "Front-end electronics for BM@N STS," Phys. Part. Nucl. **52**, 826—829 (2021). https://doi.org/10.1134/S1063779621040559
12. D. Dementev and M. Shitenkow, "Performance of STS-HCTSP with long transmission lines," CBM Progress report 2019 (Darmstadt, 2019), p. 31. https://doi.org/10.15120/GSI-2020-00904
13. D. Dementev, M. Guminski, and M. Shitenkow, "Fast data-driven readout system for the wide aperture silicon tracking system of the BM@N Experiment," Phys. Part. Nucl. **52** 830—834 (2021).
14. D. Dementev, M. O. Shitenkov, V. V. Leontiev, N. V. Sukhov, A. D. Sheremetyev, and Yu. A. Murin, "Signal/noise ratio of the silicon tracking system module of the BM@N experiment," Instrum. Exp. Tech. **66**, 19—27 (2023). https://doi.org/10.31857/S0032816223010111
15. M. J. Berger, J. S. Coursey, M. A. Zucker, and J. Chang, "Stopping-power & range tables for electrons, protons, and helium ions," NIST Standard Reference Database 124. https://doi.org/10.18434/T4NC7P
16. P. A. Zyla et al. (Particle Data Group), Prog. Theor. Exp. Phys. **2020**, 083C01 (2020).

Translated by M. Samokhina